High-order perturbative calculations of nuclear ground states: Automated evaluation of many-body diagrams

arXiv:2607.00119

Zhen Li (TU Darmstadt)

in colloaboration with Alexander Tichai (TU Darmstadt),
Achim Schwenk (TU Darmstadt),
and Nadezda A. Smirnova (LP2I Bordeaux).

Many-Body Theory: Nuclear Physics Meets Quantum Chemistry

August 24, 2026 to September 4, 2026, Mainz, Germany

Ab initio calculations for atomic nuclei

$$H|\Psi_n\rangle = E_n|\Psi_n\rangle$$

$$H = T_{\text{rel}} + \underbrace{\sum_{i<j}^{A} V_{ij}^{\text{NN}} + \sum_{i<j<k}^{A} V_{ijk}^{\text{3N}}}_{\text{from chiral EFT}}$$

- Compute nuclear properties by solving the nuclear many-body problem using systematically improvable many-body methods and inter-nucleon interactions derived from chiral effective filed theory (EFT)
- Many-body methods: QMC, HH, NCSM, Nuclear Lattice EFT, SCGF, CC, IMSRG, MBPT, $\cdots$

See *e.g.*, *Hergert et al., Front. Phys. (2020)*
Hebeler, Phys. Rept. (2021)

Chiral EFT for nuclear forces

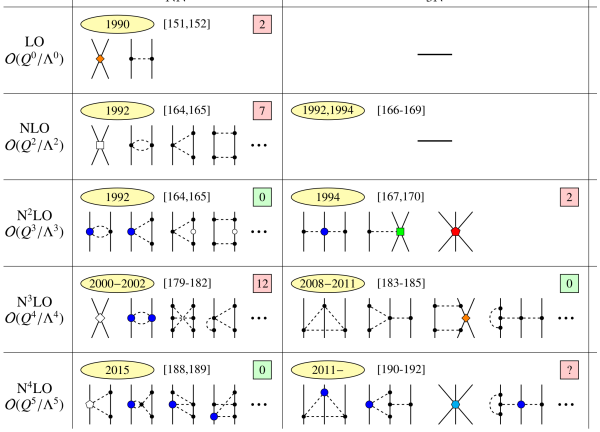

Fig. from Hebeler, Phys. Rept. (2021)

See e.g., Epelbaum et al., Rev. Mod. Phys. (2009)

Machleidt et al., Phys. Rep. (2011)

Krebs, Eur. Phys. J. A (2020)

- A low-energy effective theory of QCD with pions/nucleons (and optionally the Δ) as degrees of freedom, constrained by chiral symmetry and its breaking
- Expansion parameter $Q/\Lambda_b \simeq 1/3$
- Short-distance (high-energy) physics encoded in low-energy constants (LECs), fitted to NN scattering & few-body observables ^{2}H, ^{3}H, ...
- Systematically improvable and allows for uncertainty quantification
- Nuclear currents coupling to external probes can be derived consistently

Configuration-interaction based many-body methods for medium and heavy nuclei

- Self-consistent Green's function (SCGF) with ADC(2/3) truncation *see, e.g., Dickhoff and Barbieri PPNP (2004)*
- Coupled cluster (CC) method *see, e.g., Hagen et al., ROPP (2014)*
  - mainly CCSD and CCSD with approximate triple corrections
  - full CCSDT is challenging for practical calculations
- In-medium similarity renormalization group (IMSRG) *see Hergert et al., PR (2016); Stroberg et al., ARNPS (2019)*
  - mainly limited to particle rank-2 truncation, i.e., IMSRG(2), in practical applications
  - particle rank-3 truncation, i.e., IMSRG(3), is impossible for practical calculations
  - approximate IMSRG(3) achieved, e.g., IMSRG(3)-N^7 by Heinz et al., PRC (2021), IMSRG(3f_2) by He et al., PRC (2024), ...
- Many-body perturbation theory (MBPT) *see, e.g., Tichai et al., Front. Phys. (2020)*
  - mainly restricted to third perturbative order MBPT(3) (which is computationally cheap)
  - MBPT(≥ 4) have not been systematically investigated with nuclear interactions in atomic nuclei

See https://github.com/Takayuki-Miyagi/HartreeFock for an available MBPT(4) code by T. Miyagi

MBPT: starting Hamiltonian

- Start with a Hamiltonian after normal ordering w.r.t. a reference $|\Phi_0\rangle = \prod_{i=1}^{A} c_i^\dagger |0\rangle$

$$H = \mathcal{E}_0 + \sum_{ij} f_{ij} \mathcal{N}[c_i^\dagger c_j] + \frac{1}{(2!)^2} \sum_{ijkl} \Gamma_{ijkl} \mathcal{N}[c_i^\dagger c_j^\dagger c_l c_k] + \underbrace{\frac{1}{(3!)^2} \sum_{ijklmn} W_{ijklmn} \mathcal{N}[c_i^\dagger c_j^\dagger c_k^\dagger c_n c_m c_l]}_{\text{neglect}}$$

- Partition the Hamiltonian

$$H = H_0 + H_1 = \underbrace{\mathcal{E}_0 + \sum_i f_{ii} \{c_i^\dagger c_i\}}_{\text{unperturbed } H_0} + \underbrace{\sum_{i \neq j} f_{ij} \{c_i^\dagger c_j\} + \frac{1}{4} \sum_{ijkl} v_{ijkl} \{c_i^\dagger c_j^\dagger c_l c_k\}}_{\text{residual } H_1}$$

  with known eigenstates of H_0

$$H_0 |\Phi_m\rangle = \mathcal{E}_m |\Phi_m\rangle \,, \quad m = 0, 1, 2, \ldots, d-1 \,,$$

- $\{|\Phi_m\rangle,\ m = 0, 1, 2, \ldots, d-1\}$ span the full model space, where $\mathcal{E}_0 \leq \mathcal{E}_1 \leq \cdots \leq \mathcal{E}_{d-1}$

MBPT: Effective Hamiltonian in a subspace $\mathbb{P}$

- Cast Schrödinger equation into a selected (degenerate) subspace $\mathbb{P} \equiv \{|\Phi_m\rangle,\ m = 0, 1, 2, \ldots, d_p - 1\}$ with an effective Hamiltonian

see, e.g., Suzuki and Lee, PTP (1980)

$$H_{\text{eff}} = PH\Omega P, \qquad P \equiv \sum_{m=0}^{d_p-1} |\Phi_m\rangle\langle\Phi_m|, \qquad Q = 1 - P, \qquad H_0 P = \mathcal{E} P$$

- Solve the Bloch equation (for a degenerate $\mathbb{P}$ space) to get the wave operator Ω

$$(\mathcal{E} - H_0)\Omega P = QH_1\Omega P - Q\Omega PPH_1\Omega P$$

MBPT: Perturbative construction of the effective Hamiltonian

- Compute $\Omega = \sum_{n=0}^{\infty} \Omega^{(n)}$ perturbatively by iterating the Bloch equation *see, e.g., Suzuki and Lee, PTP (1980)*

$$\Omega^{(n+1)} = RH_1\Omega^{(n)}P - \sum_{k=1}^{n} R\Omega^{(k)}PH_1\Omega^{(n-k)}P, \quad \Omega^{(0)} = P, \quad R \equiv Q\frac{1}{\mathcal{E} - QH_0Q}Q$$

- Ground-state energy can be computed by using a one-dimensional $\mathbb{P}$ space $\{|\Phi_0\rangle\}$ with $\mathcal{E} = \mathcal{E}_0$

$$E = \langle\Phi_0|H_{\text{eff}}|\Phi_0\rangle = \sum_{n=1}^{\infty}\langle\Phi_0|H\Omega^{(n-1)}|\Phi_0\rangle = \sum_{n=1}^{\infty} E^{(n)}$$

- Wave function in full model space can be restored by

$$|\Psi\rangle = \Omega|\Phi_0\rangle = \sum_{n=0}^{\infty}\Omega^{(n)}|\Phi_0\rangle$$

- Other observables can also be evaluated

$$\langle O\rangle = \frac{\langle\Psi|O|\Psi\rangle}{\langle\Psi|\Psi\rangle}$$

MBPT: Diagrammatic formalism

- Ground-state energy corrections are

$$
\begin{aligned}
E^{(1)} &= \langle \Phi_0 | H | \Phi_0 \rangle = \mathcal{E}_0 \quad \text{(i.e., the HF energy in a HF basis)}\,, \\
E^{(2)} &= \langle \Phi_0 | H_1 R H_1 | \Phi_0 \rangle\,, \\
E^{(3)} &= \langle \Phi_0 | H_1 R H_1 R H_1 | \Phi_0 \rangle\,, \\
E^{(4)} &= \langle \Phi_0 | H_1 R H_1 R H_1 R H_1 | \Phi_0 \rangle - \langle \Phi_0 | H_1 R^2 H_1 | \Phi_0 \rangle \langle \Phi_0 | H_1 R H_1 | \Phi_0 \rangle\,, \\
&\vdots
\end{aligned}
$$

  and can be represented by linked diagrams

  see, e.g., Shavitt and Bartlett, Many-Body Methods in Chemistry and Physics: MBPT and Coupled-Cluster

- Second-order correction $E^{(2)}$ (2 diagrams in total, 1 diagram with only two-body vertices):

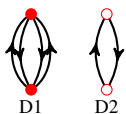

MBPT: Diagrammatic formalism

- Third-order correction $E^{(3)}$ (14 diagrams in total, 3 diagrams with only two-body vertices):

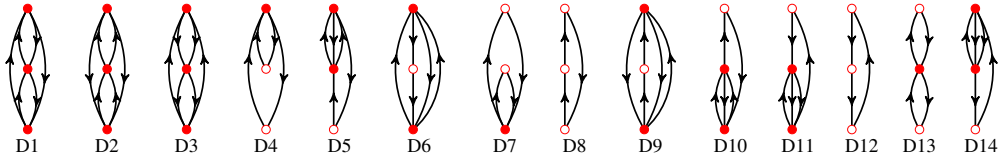

- Fourth-order correction $E^{(4)}$ (201 diagrams in total, 39 diagrams with only two-body vertices)
- Fifth-order correction $E^{(5)}$ (4704 diagrams in total, 840 diagrams with only two-body vertices)
- Diagrams for scalar operator expectations can be obtained from energy diagrams, e.g.,

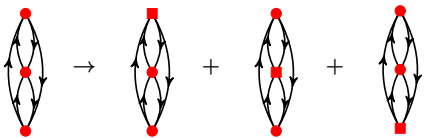

$$R^2_{\rm ch} = R^2_p + \langle r^2_{\rm p}\rangle + \langle r^2_{\rm n}\rangle \cdot \frac{N}{Z} + \langle r^2\rangle_{\rm so} + r^2_{\rm DF}$$

$$R^2_P = \frac{1}{Z}\sum_{i=1}^{Z}(\boldsymbol{r}_i^{(p)} - \boldsymbol{R}_{\rm cm})^2$$

see, e.g., Brandow, RMP (1967) and Advances in Quantum Chemistry (1977)

MBPT: difficulties of implementing MBPT(≥ 4)

- Large amount of diagrams to find, evaluate, and code
- Error-prone to do the above by hand $\rightarrow$ need automation
- Automation of diagram generation and evaluation (m-scheme)
  - J. Paldus and H.C. Wong, Comput. Phys. Commun. (1973)
  - `ADG` by P. Arthuis et al. (https://github.com/adgproject/adg)
  - tools developed in ZL's thesis (2023)
- Automation of m-scheme expression to j-scheme expression (to reduce computation cost)
  - `AMC` by Tichai, et al., EPJA (2020)
  - e.g.,

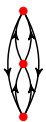

$$= \frac{1}{2^3} \sum_{h_1 h_2 p_1 p_2 p_3 p_4} \frac{\langle h_1 h_2|V|p_1 p_2\rangle\langle p_1 p_2|V|p_3 p_4\rangle\langle p_3 p_4|V|h_1 h_2\rangle}{(\varepsilon_{h_1}+\varepsilon_{h_2}-\varepsilon_{p_1}-\varepsilon_{p_2})(\varepsilon_{h_1}+\varepsilon_{h_2}-\varepsilon_{p_3}-\varepsilon_{p_4})}, \quad h_1 \equiv (n_{h_1}, l_{h_1}, j_{h_1}, m_{h_1}, t_{h_1}), \ldots \quad m\text{-scheme}$$

$$= \frac{1}{2^3} \sum_{J \tilde{h}_1 \tilde{h}_2 \tilde{p}_1 \tilde{p}_2 \tilde{p}_3 \tilde{p}_4} \sqrt{2J+1} \frac{\langle \tilde{h}_1 \tilde{h}_2; J|V|\tilde{p}_1 \tilde{p}_2; J\rangle\langle \tilde{p}_1 \tilde{p}_2; J|V|\tilde{p}_3 \tilde{p}_4; J\rangle\langle \tilde{p}_3 \tilde{p}_4; J|V|\tilde{h}_1 \tilde{h}_2; J\rangle}{(\varepsilon_{\tilde{h}_1}+\varepsilon_{\tilde{h}_2}-\varepsilon_{\tilde{p}_1}-\varepsilon_{\tilde{p}_2})(\varepsilon_{\tilde{h}_1}+\varepsilon_{\tilde{h}_2}-\varepsilon_{\tilde{p}_3}-\varepsilon_{\tilde{p}_4})}, \quad \tilde{h}_1 \equiv (n_{h_1}, l_{h_1}, j_{h_1}, t_{h_1}), \ldots \quad j\text{-scheme}$$

- Automation of computing code generation

Workflow

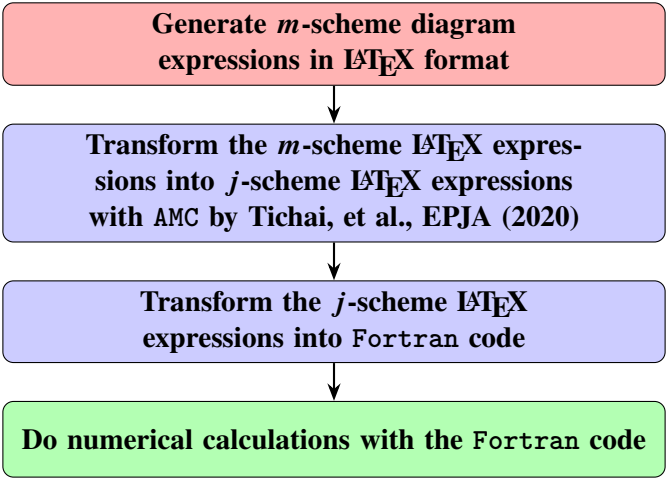
Generate m-scheme diagram expressions in LaTeX format
Transform the m-scheme LaTeX expressions into j-scheme LaTeX expressions with AMC by Tichai, et al., EPJA (2020)
Transform the j-scheme LaTeX expressions into Fortran code
Do numerical calculations with the Fortran code

Numerical benchmarks

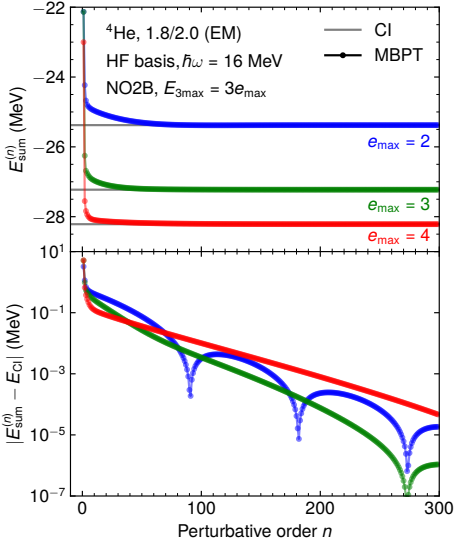

- CI: exact configuration-interaction calculation
- MBPT: iterating the recursive equation in CI basis

$$\Omega^{(n+1)} = RH_1\Omega^{(n)}P - \sum_{k=1}^{n} R\Omega^{(k)}PH_1\Omega^{(n-k)}P$$

  similar limitation as CI

- MBPT is converging to the exact CI solution for 1.8/2.0 (EM)

  see also A. Tichai et al., PLB (2016)

- Validation of generated diagrams and codes:
  diagrammatic calculations agree with the above recursive MBPT calculations

  1.8/2.0 (EM): Hebeler et al. PRC (2011)

see arXiv:2606.22341 and PRC 113 (2026) L051302 by R.Z. Hu, X. Zhen et al. for possibilities of going to larger model space

In-medium similarity renormalization group (IMSRG)

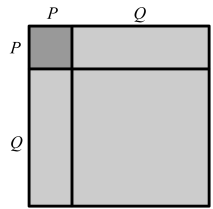

Unitary transformations $U(s)$

Decouple P space from Q space

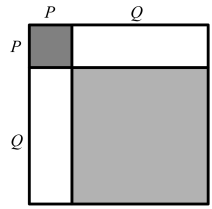

Hergert et al., Phys. Rep. (2016)
Stroberg et al., Ann. Rev. Nucl. Part. Sci. (2019)

$$H|\Psi_n\rangle = E_n|\Psi_n\rangle \qquad H_{\text{eff}}|\Psi_n^P\rangle = E_n|\Psi_n^P\rangle$$

$$H = T_{\text{rel}} + \sum_{i<j}^{A} V_{ij}^{\text{NN}} + \sum_{i<j<k}^{A} V_{ijk}^{\text{3N}} \qquad H_{\text{eff}} = [U(s)HU^{\dagger}(s)]_{s\to\infty}$$

- Large model-space eigenvalue problem is cast into a P space
- Particle-hole excitations from P to Q are encoded in the *effective* Hamiltonian
- Single-reference IMSRG: One-dimensional P space $\{|\Phi_0\rangle\} \rightarrow E_{\text{gs}} = \langle\Phi_0|H|\Phi_0\rangle = H^{(0\text{b})}$
- Valence-space IMSRG: Multi-dimensional P space $\rightarrow$ diagonalizing $H_{\text{eff}} \rightarrow$ energies and eigenstates

Multilevel truncation scheme

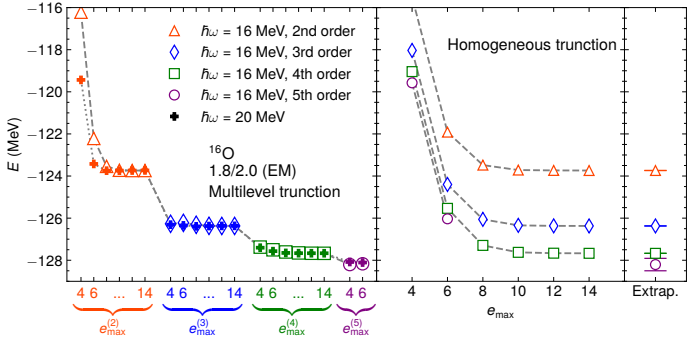

- Higher order corrections converge faster than lower orders in terms of $e_{\max}$
- A multilevel truncation is favorable to introduce higher-order corrections in smaller $e_{\max}$ (which converge faster)
- 5th-order correction (can only be computed in small $e_{\max}$) is useful under the multilevel truncation

see arXiv:2608.18975 by L. Zurek et al. for a detailed study of the balance between many-body truncation and model space truncation

Ground-state energies of selected closed-shell nuclei

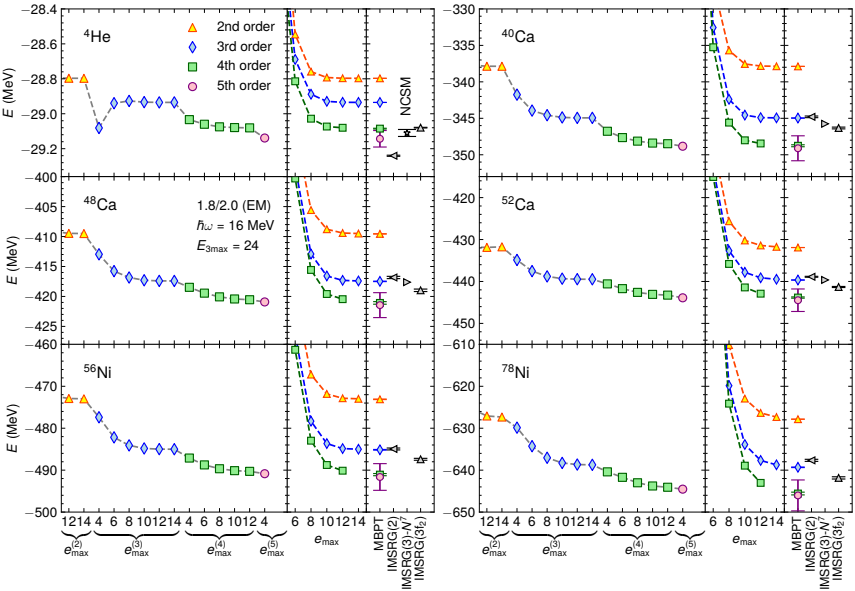

- 4th-order correction converges much faster than the 3rd order (and also the 2nd order)
- MBPT(4/5*) are very close to NCSM calculation of ^{4}He
- MBPT(4) energies are lower than IMSRG(2), IMSRG(3)-N^7, and IMSRG(3f_2) (with perturbative triples) for nuclei heavier than ^{4}He

NCSM: Hebeler, PR (2021)
IMSRG(3)-N^7: Heinz et al., PRC (2025)

Radii of some closed-shell nuclei Ca isotopes

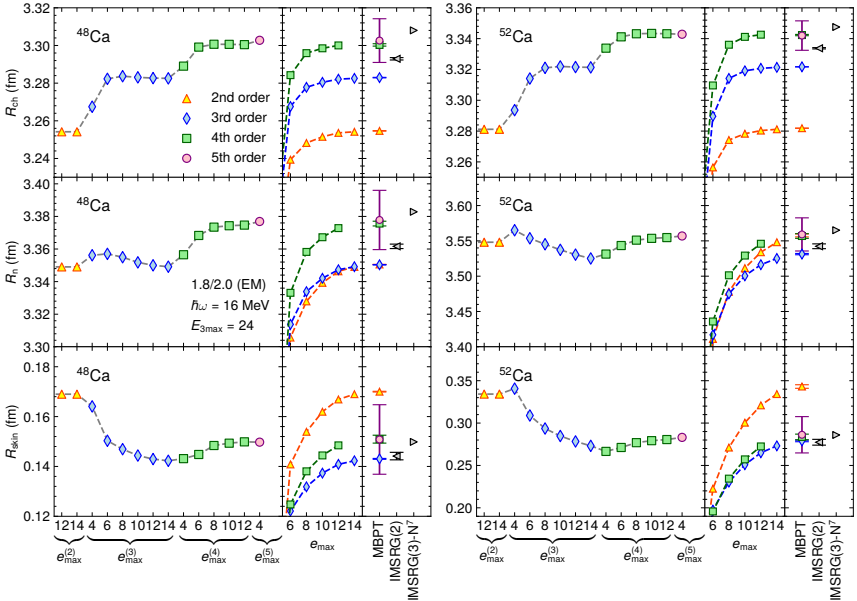

- 4th order converges faster than the 3rd order in terms of $e_{\max}$ for charge radii
- Slow convergence for neutron radii and neutron skins
- MBPT(3) results are smaller than IMSRG(2)
- MBPT(4) results are larger IMSRG(2) and smaller (or larger for R_{skin} of ^{48}Ca) than IMSRG(3)-N^7

IMSRG(3)-N^7: Heinz et al., PRC (2025)

Interaction sensitivity: ground-state energy of ^{48}Ca

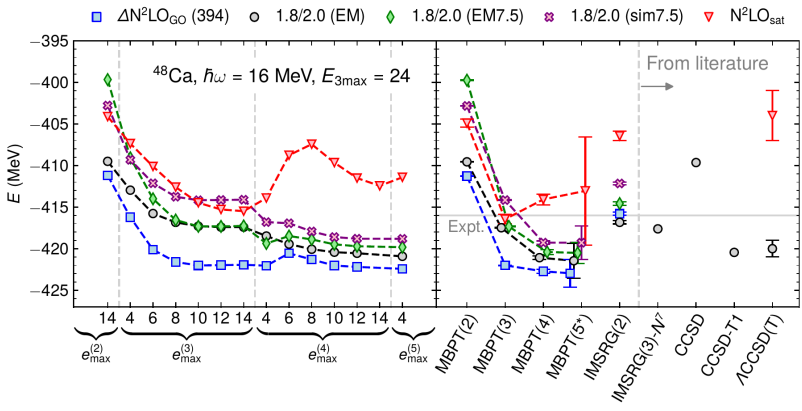

ΔN^2LO_{GO} (394): Jiang et al., PRC (2020)

1.8/2.0 (EM): Hebeler et al., PRC (2011)

1.8/2.0 (EM7.5): Arthuis et al., EPJA (2026)

1.8/2.0 (sim7.5): Arthuis et al., EPJA (2026)

N^2LO_{sat}: Ekström et al., PRC (2015)

IMSRG(3)-N^7: Heinz et al., PRC (2025)

CCSD/CCSDT-1/ΛCCSD(T): Hagen, et al., NP (2015); Bonaiti, private communication (2026); Simonis, et al., EPJA (2019)

- Slow order-by-order convergence for N^2LO_{sat}, and fast convergence for ΔN^2LO_{GO} (394)
- Fourth-order correction converges faster than the third order in terms of e_{max}
- MBPT(≥ 3) energies are lower than IMSRG(2) for all interactions
- MBPT(4) energy is closer to CCSDT-1 and ΛCCSD(T) than IMSRG(3)-N^7

Radius of ^{48}Ca

- Higher-order corrections are small compared to the differences between interactions
- Small charge radius from 1.8/2.0 (EM) compared to experiment

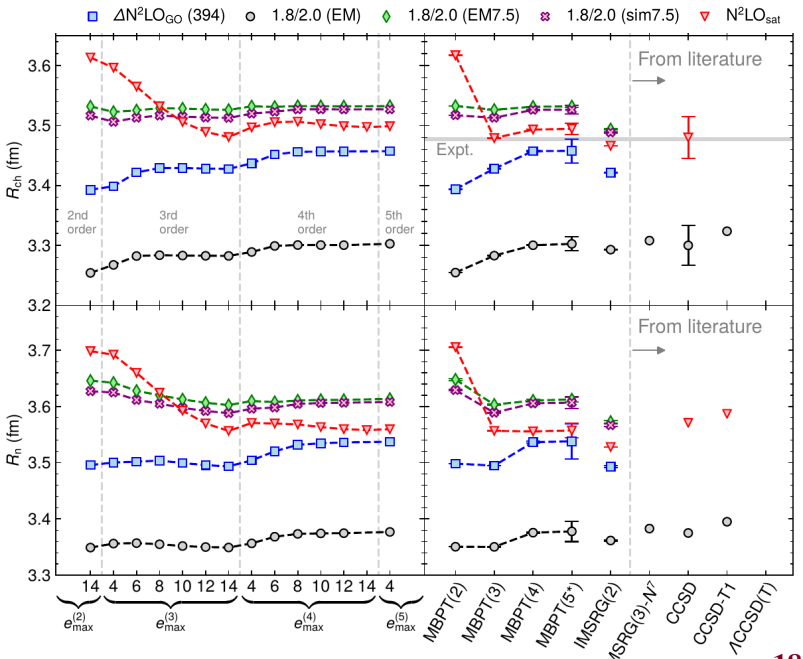

Interaction sensitivity: ratio of successive energy corrections

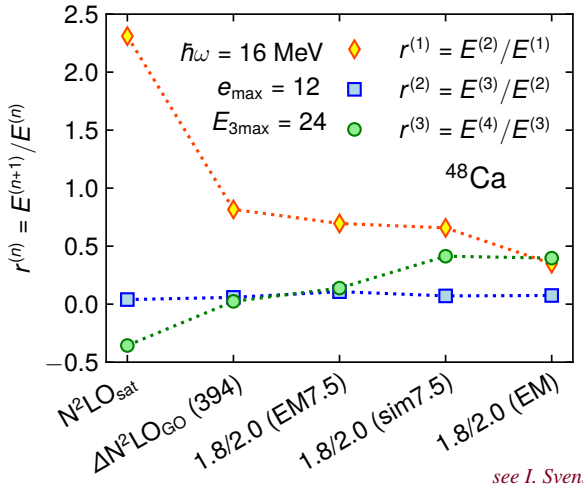

- Third-order corrections are small compared to second-order corrections
- Fourth-order corrections are in general less than half of the third-order corrections
- Ratios differ largely among different interactions;
  N^{2}LO$_{sat}$ is especially different from the others

see I. Svensson et al., PRC (2026) for uncertainty quantification of MBPT

Decomposition of fourth-order diagrams

- Singles (middle $1p1h$ excitation, 4 diag.)

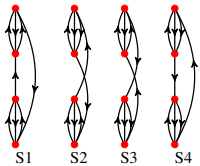

- Triples (middle $3p3h$ excitation, 16 diag.)

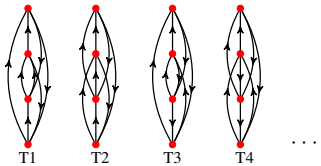

- Doubles (middle $2p2h$ excitation, 12 diag.)

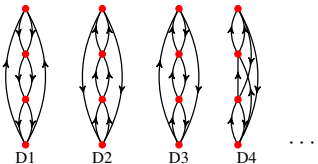

- Quadruples (middle $4p4h$ excitation, 7 diag.)

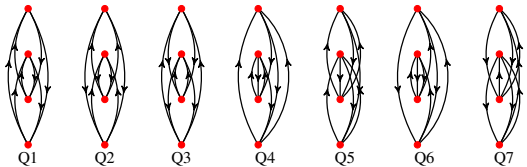

IMSRG(2) includes diagrams up to 3rd order, partial 4th order diagrams $S + D + Q_a + Q_b/2$, and higher-order ladder/ring diagrams

$$Q_a \equiv Q_1 + Q_2 + Q_3 \qquad [Q_a \text{ included in IMSRG(2)}]$$
$$Q_b \equiv Q_4 + Q_5 + Q_6 + Q_7 \qquad [Q_b/2 \text{ included in IMSRG(2)}]$$

Decomposition of $E^{(4)}$ for different nuclei with 1.8/2.0 (EM) interaction

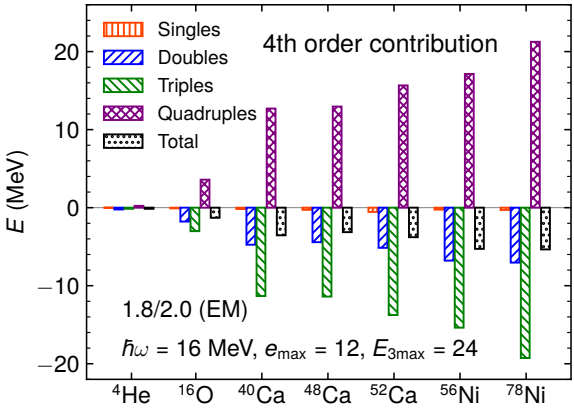

- Singles, doubles, triples are negative
- Quadruples are positive
- Singles are negligible,
  while triples and quadruples dominate
- Universal for all the nuclei considered

Decomposition of $E^{(4)}$ for ^{48}Ca with different interactions

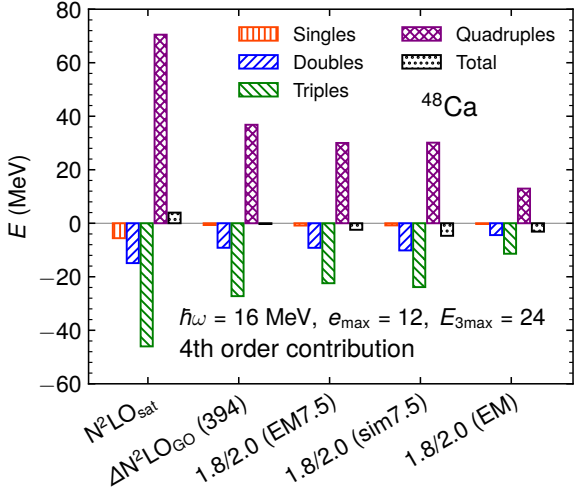

- Singles, doubles, triples are negative
- Quadruples are positive
- Singles are negligible,
  while triples and quadruples dominate
- N^2LO_{sat} produces significantly large positive quadruples,
  yielding positive 4th-order energy correction

MBPT vs. IMSRG(2)

- MBPT(2)
  → MBPT(3)
  → MBPT(3) + $S + D + Q_a + Q_b/2 + L_{5+}$
  → differ from IMSRG(2) by $\lesssim 2$ MeV, same ordering as IMSRG(2) for different interactions
- $Q_b/2$ avoids too repulsive energies when triples are not included in IMSRG(2)
- MBPT is reliable for the interactions considered (even for the relatively "harder" interaction N^2LO_{sat})

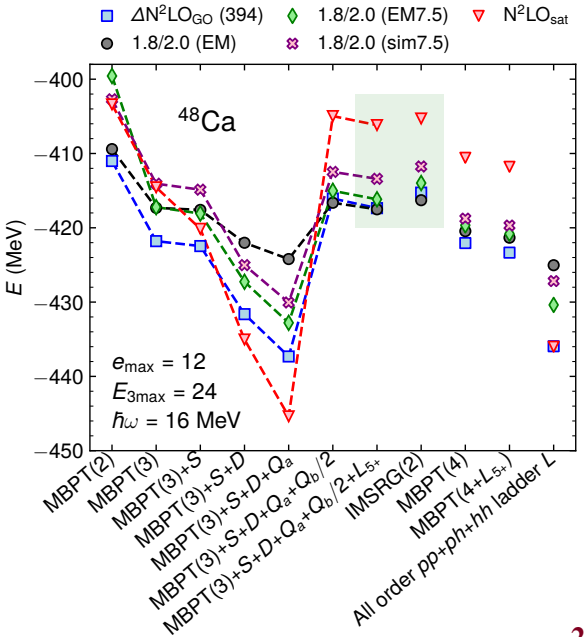

Perturbative calculation with only ladder diagrams

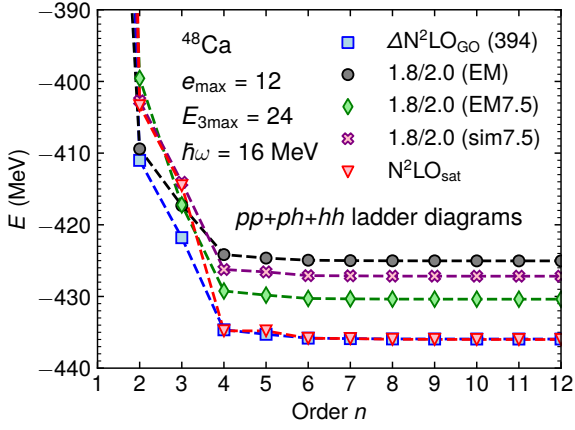

- Perturbative calculation with only ladder diagrams quickly converges
- but likely overestimates the ground-state energy

Summary

arXiv:2607.00119

- MBPT calculation up to 5th order is achieved for closed-shell nuclei, albeit the 5th order correction is only possible in small $e_{\max}$
- A comparison with the nonperturbative IMSRG(2) calculation suggests that MBPT(4) is reliable for commonly used “soft” interactions
- Therefore, MBPT(4/5*) can achieve higher precision than the traditional MBPT(3) in the calculations of atomic nuclei
- Beyond this talk:
  - VS-IMSRG calculation of nuclear beta decay of $N = 50$ neutron-rich nuclei → PRL 136 (2026) 182501 with Miyagi and Schwenk
  - VS-IMSRG calculation of $\beta\beta$ decays of ^{48}Ca → arXiv:2607.11733 with Jokiniemi and Schwenk

Summary

arXiv:2607.00119

- MBPT calculation up to 5th order is achieved for closed-shell nuclei, albeit the 5th order correction is only possible in small $e_{\max}$
- A comparison with the nonperturbative IMSRG(2) calculation suggests that MBPT(4) is reliable for commonly used “soft” interactions
- Therefore, MBPT(4/5*) can achieve higher precision than the traditional MBPT(3) in the calculations of atomic nuclei
- Beyond this talk:
  - VS-IMSRG calculation of nuclear beta decay of $N = 50$ neutron-rich nuclei → PRL 136 (2026) 182501 with Miyagi and Schwenk
  - VS-IMSRG calculation of $\beta\beta$ decays of ^{48}Ca → arXiv:2607.11733 with Jokiniemi and Schwenk

Thank you for your attention!

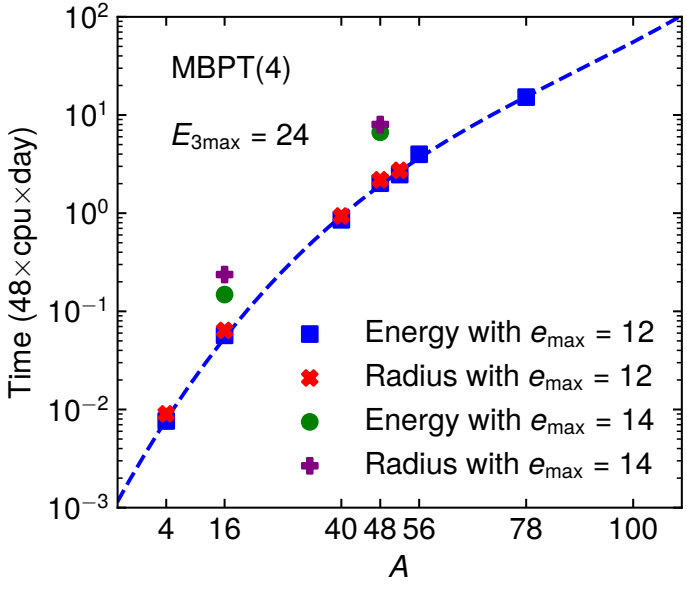
MBPT(4)
E_{3max} = 24
Energy with e_{max} = 12
Radius with e_{max} = 12
Energy with e_{max} = 14
Radius with e_{max} = 14
Time (48×cpu×day)
10^2
10^1
10^0
10^{-1}
10^{-2}
10^{-3}
4
16
40
48
56
78
100
A